OXFORD

Human Molecular Genetics, 2015, Vol. 24, No. 21 6229–6239

doi: 10.1093/hmg/ddv341
Advance Access Publication Date: 26 August 2015
Original Article

ORIGINAL ARTICLE

Intravitreal delivery of a novel AAV vector targets ON bipolar cells and restores visual function in a mouse model of complete congenital stationary night blindness

Miranda L. Scalabrino[1], Sanford L. Boye[1], Kathryn M. H. Fransen[3], Jennifer M. Noel[4], Frank M. Dyka[1], Seok Hong Min[1], Qing Ruan[1], Charles N. De Leeuw[6,7], Elizabeth M. Simpson[6,7], Ronald G. Gregg[5], Maureen A. McCall[3,4], Neal S. Peachey[8,9,10] and Shannon E. Boye[1,2,*]

[1]Department of Ophthalmology and, [2]Department of Molecular Genetics and Microbiology, University of Florida College of Medicine, Gainesville, FL 32610, USA, [3]Department of Ophthalmology and Visual Sciences, [4]Department of Anatomical Sciences and Neurobiology and, [5]Department of Biochemistry and Molecular Biology, University of Louisville, Louisville, KY 40202, USA, [6]Centre for Molecular Medicine and Therapeutics at the Child and Family Research Institute, University of British Columbia, Vancouver, BC, Canada V5Z 4H4, [7]Department of Medical Genetics, University of British Columbia, Vancouver, BC, Canada V6T 1Z3, [8]Louis Stokes Cleveland VA Medical Center, Cleveland, OH 44106, USA, [9]Cole Eye Institute, Cleveland Clinic, Cleveland, OH 44195, USA and [10]Department of Ophthalmology, Cleveland Clinic Lerner College of Medicine of Case Western Reserve University, Cleveland, OH 44195, USA

*To whom correspondence should be addressed at: University of Florida, PO Box 100284, Gainesville, FL 32610, USA. Tel: +1 3522739342; Fax: +1 3523922062; Email: shannon.boye@eye.ufl.edu

Abstract

Adeno-associated virus (AAV) effectively targets therapeutic genes to photoreceptors, pigment epithelia, Müller glia and ganglion cells of the retina. To date, no one has shown the ability to correct, with gene replacement, an inherent defect in bipolar cells (BCs), the excitatory interneurons of the retina. Targeting BCs with gene replacement has been difficult primarily due to the relative inaccessibility of BCs to standard AAV vectors. This approach would be useful for restoration of vision in patients with complete congenital stationary night blindness (CSNB1), where signaling through the ON BCs is eliminated due to mutations in their G-protein-coupled cascade genes. For example, the majority of CSNB1 patients carry a mutation in nyctalopin (*NYX*), which encodes a protein essential for proper localization of the TRPM1 cation channel required for ON BC light-evoked depolarization. As a group, CSNB1 patients have a normal electroretinogram (ERG) a-wave, indicative of photoreceptor function, but lack a b-wave due to defects in ON BC signaling. Despite retinal dysfunction, the retinas of CSNB1 patients do not degenerate. The Nyx^{nob} mouse model of CSNB1 faithfully mimics this phenotype. Here, we show that intravitreally injected, rationally designed AAV2(quadY-F +T-V) containing a novel 'Ple155' promoter drives either GFP or YFP_*Nyx* in postnatal Nyx^{nob} mice. In treated Nyx^{nob} retina, robust and targeted *Nyx* transgene expression in ON BCs partially restored the ERG b-wave and, at the cellular level, signaling in ON BCs. Our results support the potential for gene delivery to BCs and gene replacement therapy in human CSNB1.

Received: July 2, 2015. **Revised:** August 11, 2015. **Accepted:** August 17, 2015

Introduction

Retinal ON bipolar cells (ON BCs) depolarize in response to light-induced reduction of photoreceptor glutamate release and form the primary excitatory conduit between photoreceptors and retinal ganglion cells (RGCs). Mutations in genes that encode proteins involved in the ON BC metabotropic glutamate receptor 6 (mGluR6) G-protein-coupled signaling cascade are responsible for various forms of complete congenital stationary night blindness (CSNB1) (1). Patients with CSNB1 present in early childhood with impaired night vision and can be diagnosed by ERG, where they display a distinctive absence of the ON BC-driven b-wave, while maintaining a normal photoreceptor a-wave (2). CSNB1 patients also exhibit other phenotypes including severe myopia, strabismus and nystagmus (3). Mouse models harboring mutations in homologous CSNB1 genes such as *Grm6* (4–8), the non-selective cation channel TRP melastatin 1 (*Trpm1*) (9–12), the orphan G protein receptor (*Gpr179*) (13,14) and two leucine-rich repeat proteins, nyctalopin (*Nyx*) (15–17) and *Lrit3* (18,19), faithfully recapitulate the no b-wave ERG phenotype seen in CSNB1 patients and collectively will be referred to as 'nob' mice. These proteins are all localized to the dendritic tips of ON BCs, and their mouse models have been used to interrogate the role of each in the mGluR6 cascade (Fig. 1). From these studies, we know that in the absence of light, glutamate released from photoreceptors binds to the metabotropic mGluR6 (20,21) and activates a G-protein, G_o (22,23). While the exact cascade sequence remains unknown, it is clear that the initial step requires dissociation of G-protein subunits and culminates in closure of the TRPM1 cation channel (24–26). NYX is required for the correct localization of TRPM1 (27), whereas GPR179 mediates channel sensitivity (28). LRIT3 is also important for the correct localization of TRPM1 (27,29,30). Despite the disruption in ON BC signaling, mutations in these cascade proteins have no effect on retinal morphology in CSNB1 patients or respective mouse models (1). This suggests that they are good candidates for gene replacement therapy.

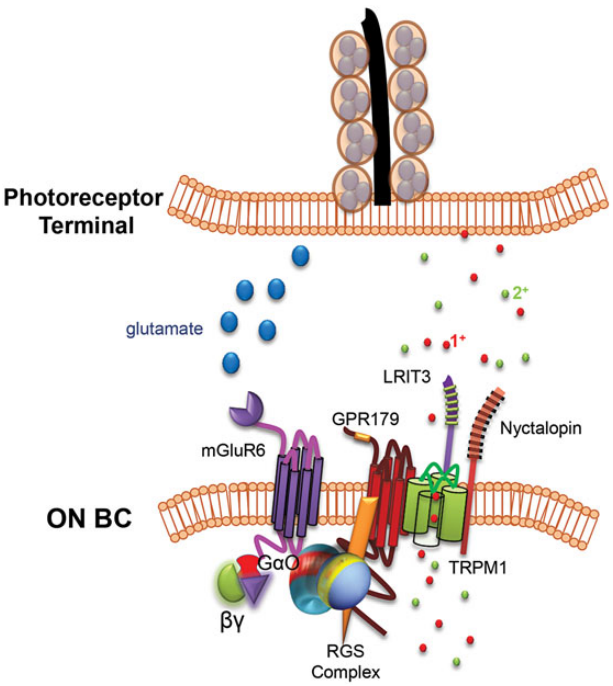

Figure 1. Glutamate cascade proteins expressed in dendritic tips of ON BCs. Glutamate released from photoreceptor terminals in the dark binds the mGluR6 metabotropic glutamate receptor and activates the alpha subunit of a heterotrimeric G-protein, $G\alpha_o$. Dissociation of G-protein subunits culminates in closure of the non-selective cation channel, TRPM1. $G\alpha_o$ is inactivated by the β subunit (β5) and by a GTPase activating the regulator of G-protein signaling complex. A leucine-rich repeat protein, NYX, is required for the correct localization of TRPM1, whereas GPR179, another G-protein receptor, mediates channel sensitivity. LRIT3 interacts with both NYX and TRPM1.

Adeno-associated virus (AAV) has demonstrated remarkable success both in clinical trials for inherited retinal disease and in a multitude of proof of concept experiments (31–37). Retinal pigment epithelium and photoreceptors are efficiently targeted by various AAV serotypes following delivery to the subretinal space. RGCs are efficiently transduced following vitreal delivery (38,39). Transduction of inner nuclear layer cell types (e.g. ON BCs) within non-degenerate retinas and selective transgene expression in ON BCs has proved challenging. This is due to the inability of most AAV serotypes to efficiently traffic to cells of the inner retina. To date, AAV has been used only to deliver xenogeneic microbial opsins, an artificial iGluR6-based optical switch, or melanopsin-derived light sensors to ON BCs, all with the goal of conferring light sensitivity to second-order neurons in mouse models lacking photoreceptors (40–44). In all instances, transgene expression was driven in ON BCs by a *Grm6* enhancer sequence fused to the SV40 promoter. Because these studies were conducted in rodent models exhibiting advanced photoreceptor degeneration, it is unclear whether the Grm6/SV40 promoter would be suitable for driving selective expression in ON BCs in non-degenerate, stationary models such as *nob* mice.

To this end, we developed a novel AAV vector and cellular promoter combination capable of driving efficient and targeted transgene expression in ON BCs of non-degenerate mouse retina following intravitreal injection. We show that AAV2 (quadY-F+T-V)-Ple155 mediates transgene expression in ON BCs and restores ON BC signaling in C57BL/6J wild type (WT) and in the Nyx^{nob} mouse model of CSNB1. This is the first demonstration that an inherent genetic defect of ON BCs can be corrected with AAV-based gene therapy. Our results have implications for the development of gene therapies for *NYX* and other forms of CSNB1 and for non-invasive optogenetic manipulation of ON BC signaling.

Results

AAV2(quadY-F+T-V)-Ple155 drives robust and targeted transgene expression in ON BCs

We previously identified an AAV2-based capsid variant capable of transducing the majority of retinal cells following intravitreal injection in mouse (39). We combined this variant with our recently described human MiniPromoter, 'Ple155', that promotes transgene expression in BCs of single-copy knock-in mice (45), and evaluated its ability to drive GFP expression in BCs of C57BL/6J (WT) and Nyx^{nob} mice following either subretinal or intravitreal injection (Fig. 2). In adult WT mouse retina, AAV2 (quadY-F+T-V)-Ple155-mediated GFP expression was targeted to BCs. Transduction by subretinal delivery was inefficient (Fig. 2A) compared with intravitreal injection in either WT or Nyx^{nob} retina (Fig. 2B and C). AAV-mediated GFP expression colocalized with protein kinase C alpha (PKCα) (Fig. 2A/C), a marker of rod BCs, as well as Purkinje cell protein 2 (PCP2) (Fig. 2B), a marker of rod and a subset of cone ON BCs and the source gene for the Ple155 MiniPromoter design (45). GFP expression was observed

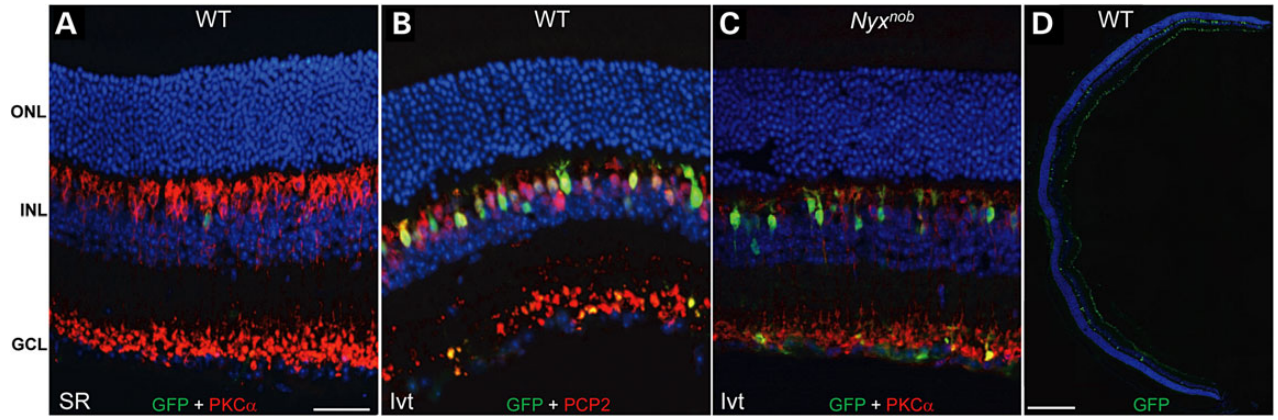

Figure 2. AAV2(quadY-F+T-V)-Ple155-mediated GFP expression (green) is restricted to ON BCs as evidenced by co-staining with either rod bipolar marker PKCα (**A** and **C**) or ON BC marker PCP2 (**B**) in red. Only minimal transduction was achieved via subretinal injection (A), but robust and targeted ON BC transduction was observed following P30 intravitreal injection in both WT (B) and *Nyx*^{nob} mice (C). Panretinal transduction of ON BCs was observed following intravitreal injection in both strains (WT shown in **D**). SR = subretinal, Ivt = intravitreal, ONL = outer nuclear layer, INL = inner nuclear layer, GCL = ganglion cell layer. Scale bars = 34 μm (A–C) and 200 μm (D).

in middle retina, with fluorescence localized to the somas and dendritic tips of ON BCs. GFP was also seen in the axon terminals of the ON BCs and was noted in some (albeit very few) RGCs in the inner retina. Intravitreal injection results in RGCs being exposed to a high concentration of vector particles. Even photoreceptor-targeted promoters such as GRK1 mediate 'off-target' GFP expression in RGCs when incorporated into AAV vectors delivered intravitreally at a high titer (39). Expression in ON BCs was widespread throughout the retinas of intravitreally injected mice (Fig. 2D). In contrast to the transduction achieved with an AAV2-based vector, intravitreal injection of AAV8(Y733F)-Ple155-GFP failed to promote transduction of ON BCs (Supplementary Material, Fig. S1).

We compared the relative abilities of Ple155 and the previously described Grm6/SV40 enhancer/promoter combination to drive transgene expression exclusively in ON BCs in a non-degenerative retina. AAV8(Y733F)-Grm6/SV40-hChR2-eGFP delivered subretinally to WT mice promoted off-target GFP expression primarily in photoreceptors (Supplementary Material, Fig. S2) (40). For its increased specificity relative to Grm6/SV40 in non-degenerate retina, the Ple155 promoter was incorporated into all further experiments.

Intravitreally injected AAV2(quadY-F+T-V)-Ple155 restores Nyctalopin expression to *Nyx*^{nob} ON BCs

Toward development of a clinically relevant approach, we examined the expression pattern of Nyctalopin (Nyx) following postnatal delivery with our AAV2(quadY-F+T-V)-Ple155 vector. We used the identical YFP_*Nyx* fusion cDNA used to generate a transgenic mouse that rescued the *Nyx*^{nob} phenotype (46). Intravitreal injection in P2 *Nyx*^{nob} mice with AAV2(quadY-F+T-V)-Ple155-YFP_*Nyx* (Fig. 3) produced widespread expression of YFP_NYX (Fig. 3A) on the dendritic tips of ON BCs (Fig. 3B and C). These data confirm reports of NYX localization to synaptic sites (15,17,46–49). There also was expression of AAV-mediated YFP_NYX in ON BC soma and axon terminals. These locations are likely to be ectopic expression due to over-expression by AAV within some ON BCs. The number of transduced ON BCs per P2-treated retina was quantified relative to the total number of ON BCs (determined by anti-PCP2 co-expression) in representative cross sections by three independent observers. The mean percentage of ON BC transduction in P2-treated *Nyx*^{nob} mice was 21.5%. Intravitreal injections in P30 WT and *Nyx*^{nob} mice (Fig. 3D and E) produced targeted expression in ON BCs, although the percentage was markedly lower compared with the P2 injections.

Nyctalopin gene replacement in *Nyx*^{nob} mice partially rescues the electroretinogram (ERG) b-wave

We evaluated the extent of ON BC function within the entire retina using the ERG. In *Nyx*^{nob} mice treated at P2, ERGs were recorded at P32. ERG b-wave responses from eyes injected with AAV2(quadY-F+T-V)-Ple155-YFP_*Nyx* were compared with untreated contralateral eyes or eyes injected with control vector, AAV2(quadY-F+T-V)-Ple155-GFP. The dark-adapted ERG responses recorded from untreated *Nyx*^{nob} control eyes (Fig. 4Ai, red tracings) were identical to previous reports (16,46). These ERGs had an overall negative polarity. In comparison, dark-adapted ERG responses in all P2 AAV-treated *Nyx*^{nob} eyes had a clear positive component (Fig. 4Ai, black tracings). Arrows indicate the ERG response components restored by AAV treatment. These data reflect a rescue of signaling through rod ON BCs. Rescue was most easily seen in response to low-luminance stimuli (e.g. −3.6 to −2.4 log cd s/m^2), where the untreated *Nyx*^{nob} ERG is essentially flat. Figure 4B summarizes the magnitude of the rescue of the dark-adapted b-wave to the −2.4 log cd s/m^2 stimulus. There was no measurable b-wave response from untreated or AAV-GFP-treated eyes (Fig. 4B). ERG improvements were significant ($P < 0.000001$). As might be expected from the limited expression in *Nyx*^{nob} mice injected with AAV2(quadY-F+T-V)-Ple155-YFP_*Nyx* at P30, we found no rescue of their ERG b-wave (data not shown, $n = 5$ retinas).

The dark-adapted responses indicate that AAV treatment rescued function in rod ON BCs. To determine if cone ON BCs were similarly affected, we recorded light-adapted ERGs with stimuli superimposed upon a steady rod-desensitizing field. Again, cone ERGs recorded from *Nyx*^{nob} control eyes were identical to previous reports (16,46,50). Figure 4Aii illustrates the light-adapted ERG responses from a mouse with a large rescue effect. Arrows again indicate the response component restored by AAV treatment. As in the example, the ERGs in AAV-treated eyes included components that resemble WT, including a waveform 'deflection' (oscillatory potential). None of these were present in untreated eyes. Finally, the magnitude of the light-adapted ERG correlated with the magnitude of dark-adapted b-wave ($r = 0.92$).

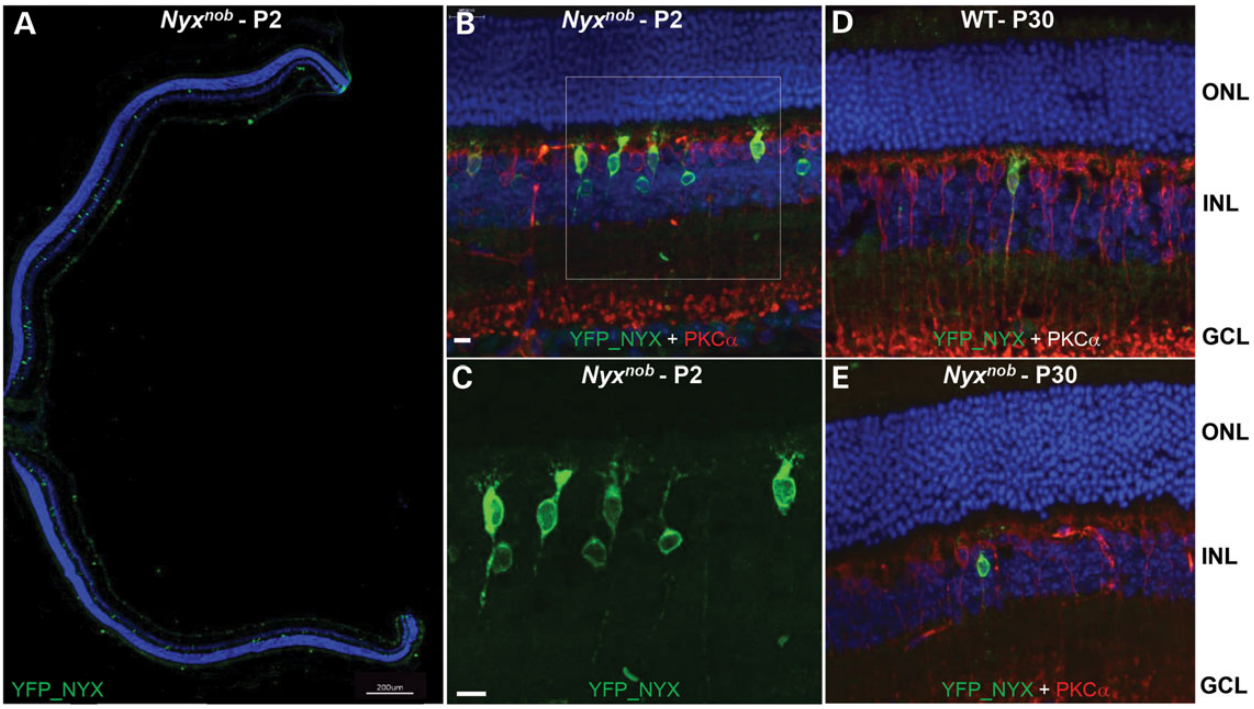

Figure 3. Intravitreal AAV2(quadY-F+T-V)-Ple155-YFP_*Nyx* transduction (green, GFP antibody) is restricted to ON BCs (red, PKCα antibody). Widespread ON BC transduction is observed in whole eyecups of P2-injected *Nyx*^{nob} mice (**A**). Intraocular injection at P2 promoted robust transduction of ON BCs in both strains (*Nyx*^{nob} mouse shown) (**B** and **C**). High magnification (white box) reveals YFP_NYX expression in cell bodies and dendritic tips of ON BCs (C). Minimal YFP_NYX expression was observed following intravitreal injection in P30 WT or *Nyx*^{nob} mice (**D** and **E**). ONL = outer nuclear layer, INL = inner nuclear layer, GCL = ganglion cell layer. Scale bars = 17 μm (A–D) and 200 μm (E).

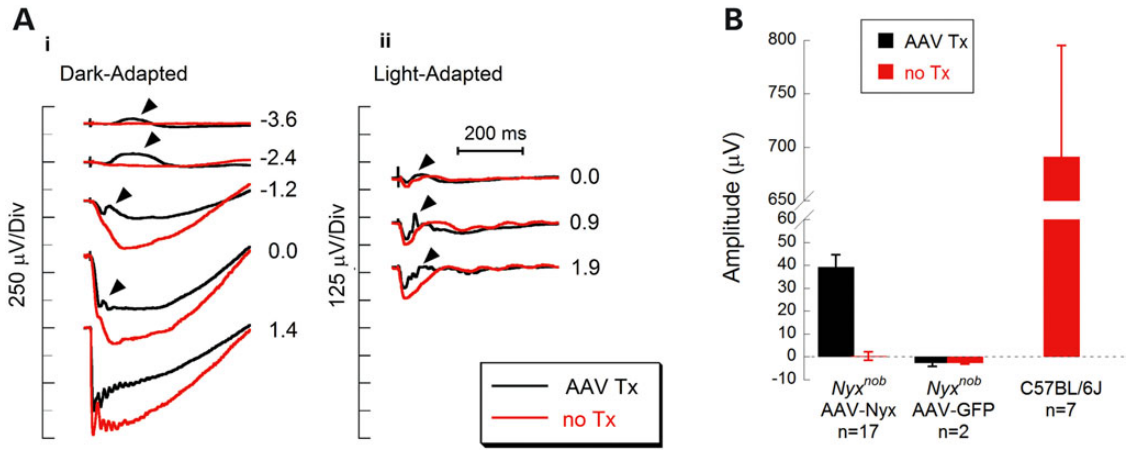

Figure 4. Electroretinographic analysis of AAV2(quadY-F+T-V)-Ple155-YFP_*Nyx*-treated, AAV2(quadY-F+T-V)-Ple155-GFP-treated and untreated *Nyx*^{nob} mice. Representative dark-adapted (**A**, left) and light-adapted (A, right) ERGs obtained from the two eyes of an individual mouse. Red traces were recorded from the untreated eye, while black traces were recorded from eye in which AAV-YFP_*Nyx* was injected. Note the presence of a positive signal (arrowheads) in the treated responses, which was not present in the responses obtained from the untreated eye. Values to the right of each pair of waveforms indicate strobe flash luminance in log cd sec/m^2. The average positive response measured at 100 ms after stimulus presentation from AAV-YFP_*Nyx* (black) and untreated (red) eyes to a −2.4 log cd sec/m^2 stimulus (**B**). The left and right pairs of bars compare responses from eyes treated with AAV-YFP_*Nyx* and AAV-GFP, respectively. Error bars report standard error of the mean. Div = division.

Gene replacement restores TRPM1 localization to dendritic tips of ON BCs and completely rescues ON BC TRPM1 channel gating

We previously showed that the expression of TRPM1 is lost in *Nyx*^{nob} mice (27). Although the function of NYX is still incompletely understood, it is clearly required to localize TRPM1 to the membrane of ON BC dendritic tips. The expression of YFP_NYX and TRPM1 (Fig. 5) in whole-mount retina from an AAV-treated *Nyx*^{nob} mouse shows that many ON BCs that express YFP_NYX (green) also express TRPM1 (red). As previously noted for TRPM1, expression is found both in ON BC cell bodies as well as on their dendritic tips (Fig. 5A). Co-expression is appreciable in single ON BCs (Fig. 5B), with robust YFP_NYX and TRPM1 expression.

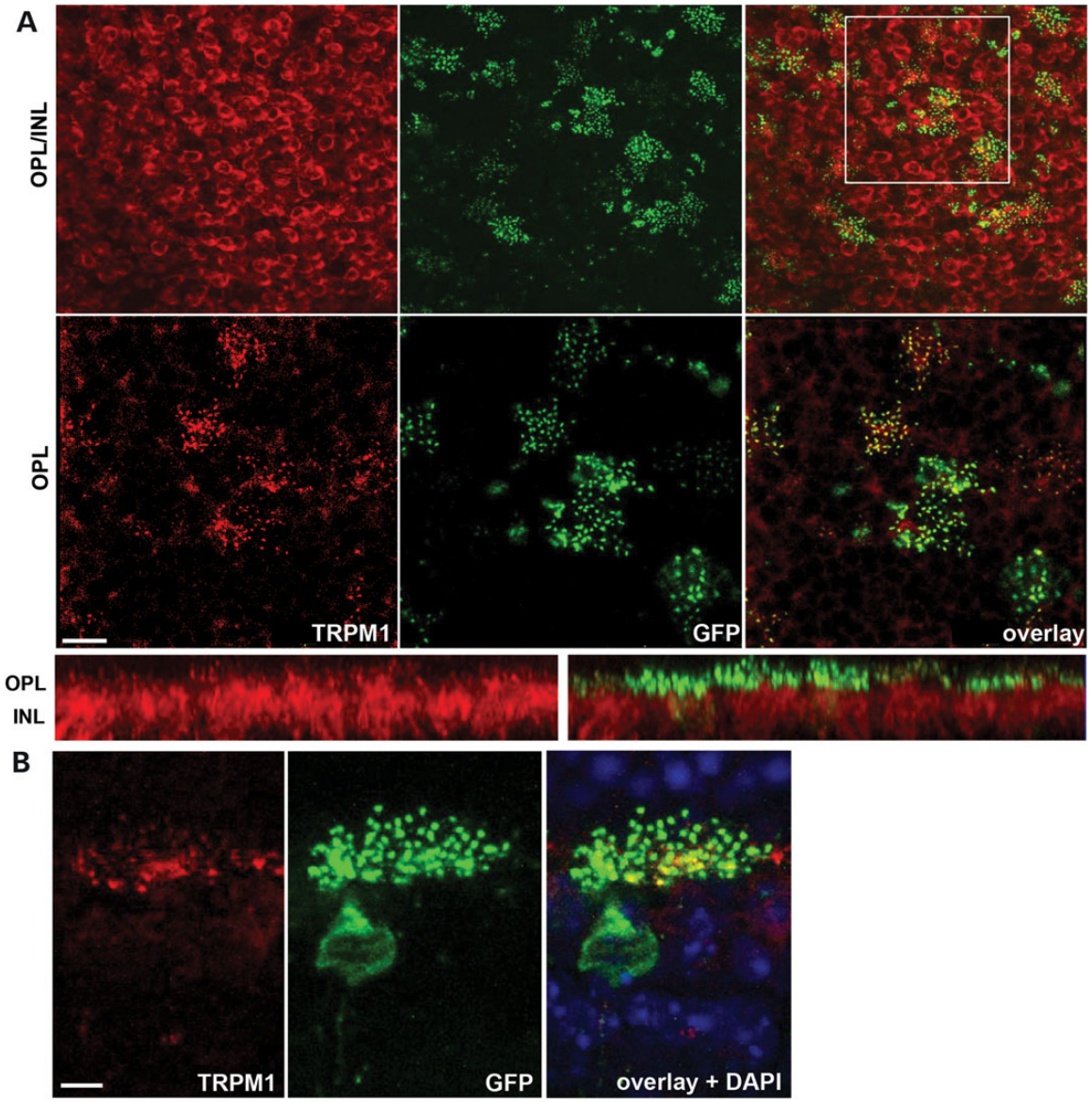

Figure 5. TRPM1 localization is restored to membranes of ON BC dendritic tips in treated Nyx^{nob} mice. Top-down view of treated retina showing TRPM1 (red) and YFP_NYX (green, GFP antibody) in cell bodies (**A**, top row) and dendritic tips (A, middle row). Dendritic tip colocalization is also shown in retinal cross section (A, bottom row) and a representative ON BC at high magnification (**B**). OPL = outer plexiform layer, INL = inner nuclear layer. Scale bars = 10 μm (A) and 5 μm (B).

ON BCs expressing YFP_NYX were targeted in retinal slices for whole-cell patch-clamp recordings and subsequently filled with sulforhodamine for morphological identification (Fig. 6A). Exogenous application of capsaicin, which directly gates the TRPM1 channel, resulted in robust outward currents in WT and AAV-treated Nyx^{nob} rod ON BCs (Fig. 6B). In contrast, only a small outward current was evoked in Nyx^{nob} rod ON BCs lacking YFP_NYX expression (Fig. 6B). This outward current is similar to residual currents recorded in $Trpm1^{-/-}$ ON rod BCs (28). The summary data show that the response amplitudes of Nyx^{nob} rod ON BCs expressing AAV-mediated YFP_NYX are similar to WT and differ significantly from rod ON BCs without YFP_NYX, some of which were recorded in the same retinas (Fig. 6C).

AAV-mediated *Nyx* transcript is present in treated mice

To determine the relative level of AAV-mediated YFP_*Nyx* transcript in early (P2) versus late (P30) treated Nyx^{nob} mice, we performed quantitative reverse transcriptase-polymerase chain reaction (qRT-PCR) on RNA extracted from P2- and P30-treated Nyx^{nob} retinas, as well as age-matched uninjected controls (retinas were extracted 30 days post-injection). Primers were designed to flank the 3′ *Nyx* gene and 5′ SV40 polyA signal with the probe binding within the first quarter of the amplicon (Table 1). Polymerase chain reaction (PCR) produced the appropriately sized amplicon in AAV-treated Nyx^{nob} retina, but not in untreated Nyx^{nob} or C57BL/6J retinas as expected (data not shown). AAV-mediated YFP_*Nyx* transcript was present in both P2- and P30-injected retinas and was normalized to *Gapdh* for comparison (Fig. 7). Despite the relatively low number of ON BCs expressing YFP_NYX in P30-treated mice (Fig. 3), YFP_*Nyx* transcript was relatively more abundant in P30- than P2-treated Nyx^{nob} mice (Fig. 7). The presence of transcript in P30-treated sample suggests efficient transgene delivery and that the hurdle to achieving robust NYX expression in P30-treated Nyx^{nob} mice is likely to be occurring post-transcription.

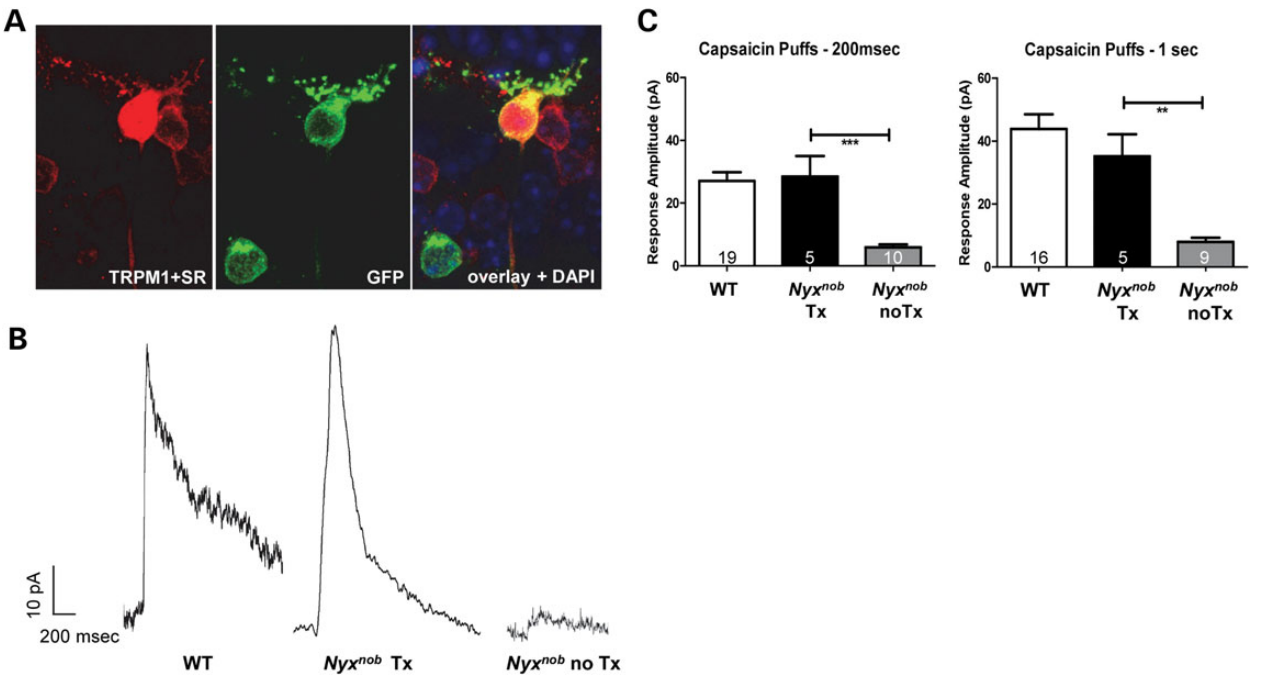

Figure 6. ON BC signaling is restored following AAV treatment in Nyx^{nob} mice. A representative rod BC expressing AAV-mediated YFP_NYX and properly localized TRPM1 was targeted for whole-cell patch-clamp recording and filled with sulforhodamine B (**A**). Capsaicin (10 μM), a TRPM1 agonist, was puffed onto the rod BC dendrites to gate the opening of the TRPM1 channel. $V_{hold} = 50$ mV. Representative current recordings from WT rod BC, AAV-treated and untreated rod BCs from Nyx^{nob} mice reveal full restoration of ON BC signaling following treatment (**B**). Capsaicin was puffed onto rod BC dendrites for 200 ms and 1 s durations. Current responses were recorded from each cell and then averaged (**C**).

Table 1. qRT-PCR primers/probe

Primer name	Sequence 5′ to 3′
GAPDH FWD	AATGGTGAAGGTCGGTGTG
GAPDH REV	GTGGAGTCATACTGGAACATGTAG
GAPDH probe	6-FAM/TGCAAATGG/ZEN/CAGCCCTGGTG/3IABkFQ
AAV-NYX FWD	CCATGCAGTGATGGTCTT
AAV-NYX REV	CATCAAGTACTTATCATGTCTGG
AAV-NYX probe	6-FAM/TCTTCACCT/ZEN/CTTGCGTCTTGCTCA/3IABkFQ

Probes are double-quenched using a 5′ 6-FAM fluorophore, 3′ IBFQ quencher and inner ZEN quencher, all trademark Integrated DNA Technologies.

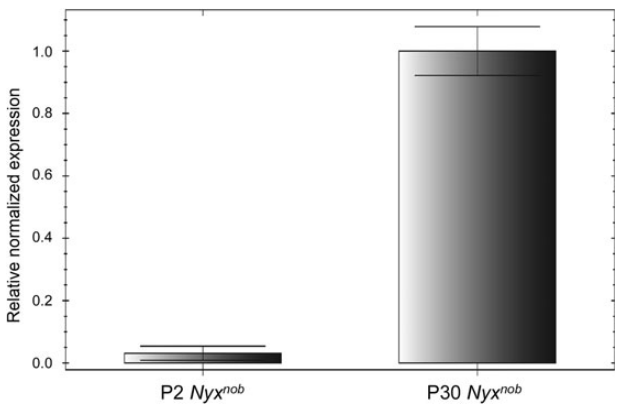

Figure 7. YFP_NYX mRNA is detectable in both early (P2)- and late (P30)-treated Nyx^{nob} retinal extracts through qRT-PCR. Standard deviations were calculated from three replicate reactions performed for each sample.

Discussion

Coordinated interaction of proteins within the mGluR6/GRM6 cascade ensures maintenance of a functional photoreceptor to ON bipolar synapse (Fig. 1). Binding of glutamate to GRM6 in the dark keeps the TRPM1 cation channel closed. In response to light, TRPM1 channels reopen, causing depolarization of ON BCs and the formation of the ERG b-wave. Proper localization of TRPM1 to the dendritic tip membrane depends on expression of NYX, although the TRPM1 protein remains expressed in the ON BC somas of Nyx^{nob} mice (27,29). While there is conflicting evidence, TRPM1 expression also may require expression of GRM6 (7,29). Finally, the absence of LRIT3 also leads to an absence of TRPM1 in dendritic tips (30), but it is not known if this is a direct consequence or results from a change in NYX expression.

Our finding that AAV2(quadY-F+T-V)-Ple155-mediated YFP_NYX expression restored TRPM1 expression to the membrane of ON BC dendritic tips in AAV-treated Nyx^{nob} mice is consistent with previous results (46). In addition, we show that this restoration of properly localized TRPM1 to the dendritic tips of rod BCs corresponds to full restoration of the rod BC's response to TRPM1 agonist, capsaicin. At the level of the entire retinal response, AAV2(quadY-F+T-V)-Ple155-mediated YFP_NYX expression partially restores the ERG b-wave in treated Nyx^{nob} mice. The mean b-wave amplitude in P2-treated eyes was ~40 μV, while age-matched C57BL/6J responses are ~675 μV (51). The fact that we observed full restoration of single-cell response amplitudes is consistent with our immunohistological results that ~22% of ON BCs expressed AAV-mediated YFP_NYX. Taken together, the data indicate that the subset of infected ON BC cells are responsible for the b-wave response.

Early (P2) and late (P30) intravitreal injection of AAV2(quadY-F+T-V)-Ple155 mediates robust and targeted GFP expression in both WT and Nyx^{nob} mice. In contrast, only early injection efficiently drives NYX expression in both strains. Not surprisingly, the ERG b-wave was not restored in Nyx^{nob} mice following the late treatment (data not shown). The treatment at P5 promoted relatively less expression than that seen following P2 treatment with ~3% of ON BCs expressing YFP_NYX (data not shown). These results suggest that supplementation of an ON BC-specific transgene is most effective when delivered, while BCs are still differentiating (52,53).

There are several possible reasons why it is difficult to express NYX in P30-treated mice. Optogenetic protein expression studies using intravitreal injection requires very high titer virus (41–44) to obtain widespread ON BC infection. Indeed, we observed that therapeutic effects were achieved when vector was delivered at 2.5×10^{13} vg/mL but not at 3.8×10^{12} vg/mL (data not shown). Thus, more viral particles may be required to make it through the barriers of the inner limiting membrane and plexiform layers to achieve sufficient transduction in the inner nuclear layer. However, the fact that AAV-mediated *Nyx* message was present in retinas injected at either P2 or P30 suggests that inefficient targeting of the transgene to ON BCs is not the cause. Indeed, transcript levels were higher in P30-treated mice, a result attributed at least in part to the larger number of ON BCs available for transduction in the fully differentiated, P30 rodent retina (52,53). Additionally, robust GFP expression mediated by AAV2(quadY-F+T-V)-Ple155 was achieved following the injection at P30. This suggests that AAV2(quadY-F+T-V) effectively transduced ON BCs at both ages, the Ple155 promoter was active and that the hurdle to achieving efficient NYX expression/therapy in older mice may be post-transcriptional.

Based on our results, it is clear that more work needs to be done to develop this strategy into a clinically translatable therapy. It is interesting to consider whether the window of therapy can be extended and if treatment, whether early or late, will resolve other phenotypes that accompany CSNB1. It is well known that the visual experience can impact synaptic function (54). For example, dark rearing disrupts GRM6 localization in cone ON BC dendritic tips (55). The absence of a functional ON pathway also affects eye development, leading to high myopia in CSNB1 patients (3) and increased susceptibility to form-deprivation myopia in mouse models with ON pathway defects (56,57), a phenotype suggested to result from decreased dopamine metabolism/turnover within the retina (56,57). ON pathway defects also lead to reduced contrast sensitivity and cortical orientation selectivity (58). Taken together, it is tempting to speculate that expression of ON BC proteins such as NYX is developmentally regulated at the translational or post-translational level.

In conclusion, this study shows for the first time that postnatal delivery of an ON BC-specific gene via AAV is capable of restoring ON BC signaling in a mouse model of CSNB1. Further improvements are needed, however, to extend the window of therapy.

Materials and Methods

Design and construction of 'Ple155' MiniPromoter

Overview methods on Pleiades Promoter design have been previously published (59). For the *PCP2* gene, a 1652 bp MiniPromoter was derived from two alternative promoters, which are annotated in the UCSC Genome Browser (version GRCh38/hg38). The basal promoter sequence (Prom1) generates transcript variant 1. A downstream alternative promoter (Prom2), located in intron 1 of transcript variant 1, generates the transcript variant 2. To avoid the conflict of two transcription start sites, the Prom2 sequence was added 5′ of the Prom1 sequence and in reverse orientation from the natural genomic configuration. Expression in the eye and brain of knock-in mice containing Ple155 driving *lacZ* had been characterized previously (45).

Table 2. PCR primers for Ple155 MiniPromoter design

Primer name	Sequence[a]
PCP2-X_OL_V1	**TTATTTGAAATGGGGTTAGTATAGA**
PCP2-X_OR_V1	**TGCCATTCCAGATGATAATCTA**
PCP2-ABD_P1R_MluI_V1	ACGT ACGCGT *TGGACTCCAGTCACTTTTC*
PCP2-BD_P1L_V1	*GGACACTTCATTGGCATAG TATGCCAATGAAGTGTCC*
PCP2-B_P2R_V1	GGATCAGGAGGAGAAGAC
PCP2-B_P2L_SacI_V1	ACGT GAGCTC TCAGCAGATTGAAGAAGC

[a]Bold, sequence matching human genome; italics, sequence matching Prom1; underlined, sequence matching Prom2; and black, non-genomic sequence containing restriction enzyme sites for subcloning.

PCR primers were designed to amplify selected regulatory regions (Table 2). Briefly, human genomic DNA was amplified using PCP-X_OL_V1 and PCP2-X_OR_V1, generating a contiguous 4500 bp PCR product containing all the regulatory regions of interest. To create the Ple155 MiniPromoter, two smaller regions were further amplified and a fusion PCR product generated as follows. Using the initial 4500 bp PCR product, primers PCP2-ABD_P1R_MluI_V1 and PCP2-BD_P1L_V1 were used to amplify the Prom1 region. Primers PCP2-B_P2R_V1 and PCP2-B_P2L_SacI_V1 were used to generate the Prom2 region. Subsequently, both Prom PCR products were used along with primers PCP2-ABD_P1R_MluI_V1 and PCP-2B_P2L_SacI_V1 to generate a fusion PCR product containing the entire MiniPromoter, which was subcloned using the *MluI*/*Sac*I sites in the multiple cloning site of the pEMS1313 backbone vector (59) to yield the pEMS1626 plasmid (45). Additional information and constructs are available from AddGene (www.addgene.org).

Construction of AAV vectors

Recombinant AAV vector plasmids containing Ple155-GFP and Ple155-YFP_NYX were engineered as follows. NYX fused to enhanced YFP (YFP_NYX) was PCR amplified out of the original transgenic clone prGABAcp1-YFP_NYX-rb456 (46). It was then inserted into a subcloning vector and fully sequenced. The YFP_NYX fragment was then cloned into pTR-mGrm6/SV40-hChR2_GFP, described in Dorodouchi *et al.* (40), using *Hind*III and *Not*I restriction enzymes. From there, YFP_NYX was moved via *Eag*I restriction site into pTR-UF-SB (60) to generate pTR-CBA-YFP_NYX. To generate pTR-Ple155-YFP_NYX, the CBA plasmid was then digested with *Not*I and the resulting YFP_NYX fragment cloned into pTR-Ple155-GFP, resulting in pTR-Ple155-YFP_NYX. pTR-Ple155-YFP_NYX and pTR-Ple155-GFP were packaged into either AAV2(quadY-F+T-V) or AAV8(Y733F). Additionally, pTR-mGrm6/SV40-hChR2_GFP packaged in AAV8(Y733F) was utilized (40). All vectors were packaged, purified and tittered according to previously published methods (61,62). Resulting titers of each virus were as follows: AAV2(quadY-F+T-V) Ple155-hGFP, 4.8×10^{13} vg/mL; AAV2(quadY-F+T-V) Ple155-YFP_NYX, 2.5×10^{13} vg/mL; AAV8(Y733F)-Ple155-hGFP, 1.2×10^{13} vg/mL; and AAV8(733)-Grm6/SV40-hChr2-GFP, 2.9×10^{12}.

Animals and injection methods

C57BL/6J (purchased from Jackson Laboratory) and Nyx^{nob} mice on a C57BL/6J background were handled according to the statement for the use of animals in Ophthalmic and Vision Research of the Association of Research in Vision and Ophthalmology and the guidelines of the Institutional Animal Care and Use Committees at the University of Florida, University of Louisville and the Cleveland Clinic. One hour prior to P30 injections, eyes were dilated with 1% atropine, followed by 2.5% phenylephrine (both Akorn, Inc., Lake Forest, IL). Mice were then anesthetized with ketamine (72 mg/kg)/xylazine (4 mg/kg) (Phoenix Pharmaceutical, St. Joseph, MO). Trans-corneal subretinal injections of virus (1 µl) were performed using a 33-gauge blunt needle on a Hamilton syringe. Trans-scleral intravitreal injections (1 µl) were done using a 33-gauge beveled needle on a Hamilton syringe. P2 mice were anesthetized on ice, and virus was delivered intraocularly (0.5 µl) using a 34-gauge beveled needle on a Hamilton syringe. Vectors were delivered undiluted in all cases.

Electroretinogram

After overnight dark adaptation, mice were anesthetized with a solution of ketamine (80 mg/kg) and xylazine (16 mg/kg). Eye drops were used to dilate the pupils (1% tropicamide and 2.5% phenylephrine HCl) and to anesthetize the corneal surface (1% proparacaine HCl). A pair of stainless steel wire electrodes was used to record ERGs from each corneal surface. These active leads were referenced to a needle electrode placed in the cheek. A second needle electrode placed in the tail served as the ground lead. ERGs were recorded using an LKC (Gaithersburg, MD) UTAS E-3000 signal averaging system. Responses evoked by ganzfeld strobe flash stimuli were band-pass filtered (0.03–1000 Hz), amplified, averaged and stored.

The Nyx^{nob} ERG is comprised primarily of response components generated by photoreceptors (a-wave), Müller glial cells (slow PIII) and hyperpolarizing BCs (50), but is missing the positive polarity component generated by depolarizing BCs (DBCs) (16). Because we were uncertain how AAV might impact the ERG waveform of treated mice, we repeated certain stimulus conditions multiple times for each mouse, to allow us to appreciate a consistent waveform change. With that exception, the recording protocol was comparable with that used for other mouse models. In each recording session, we began with dark-adapted responses to low-luminance stimuli and increased flash luminance as the session proceeded. Stimuli were presented in order of increasing luminance and ranged in flash luminance from −3.6 to 2.1 log cd s/m^2. After dark-adapted recordings were complete, cone ERGs were isolated by superimposing stimuli upon a steady adapting field (20 cd/m^2). Flash luminance ranged from −0.8 to 1.9 log cd s/m^2. All Nyx^{nob} mice intraocularly injected at P2 with AAV-*Nyx* ($n = 17$) were analyzed by ERG.

Tissue preparation, immunohistochemistry and microscopy

Four weeks post-injection, the limbi of treated and untreated Nyx^{nob} eyes were marked with ink at the 12 o'clock position, facilitating orientation. They were immediately enucleated, perforated with a needle through the cornea and stored overnight at 4°C in 4% paraformaldehyde. Cornea and lens were removed, and the eye cup was incubated in 30% sucrose solution for ~3 h at 4°C before being cryoprotected in Optimal Cutting Temperature media (Sakura Finetek USA, Inc., Torrance, CA). Twelve-micron sections were cut using a Leica cryostat (Leica CM3050 S, Wetzlar, Germany) and stored at −20°C. Retinal sections were immunostained according to previously described methods (63). Briefly, sections were brought to room temperature, rinsed with 1× phosphate-buffered saline (PBS), blocked with 0.5% Triton-X100 and 1% bovine serum albumin (BSA) for 1 h each and then incubated overnight at 4°C with primary antibodies in 3% Triton+1% BSA. Primary antibodies included rabbit polyclonal anti-GFP, which also labels YFP (1:1000, generously provided by Dr Clay Smith), 1:200 mouse monoclonal anti-PKCα (Santa Cruz, Dallas, TX) or 1:500 anti-PCP2 (Santa Cruz). After incubation with primary antibody, slides were rinsed with 1× PBS and then incubated at room temperature for 1 h with respective Alexa Fluor secondary antibodies (1:500) in 1× PBS (Invitrogen, Eugene, Oregon). Slides were then rinsed with 1× PBS, mounted with 4′,6-diamidino-2-phenylindole (DAPI)-containing SlowFade mounting media (Thermo Fisher Scientific, Waltham, MA) and coverslipped. High-magnification (20× or 40×) images were obtained via spinning disk confocal microscopy (Nikon Eclipse TE2000 microscope equipped with Perkin Elmer Ultraview Modular Laser System and Hamamatsu O-RCA-R2 camera). Tiled images (10×) of eyecups were obtained with a Keyence BZ-900E fluorescent microscope. Cell counts were performed on 40× images taken from four identical locations in optic nerve-containing eyecups. Far superior, superior/central, inferior/central and far inferior areas were sampled.

Retina pieces that were not sliced for patch-clamp recording were incubated in 4% paraformaldehyde for 20 min. Directly after the conclusion of patch-clamp experiments, retinal slices were incubated in 4% paraformaldehyde for 20 min at room temperature. The retina pieces were then rinsed in 1× PBS (3 × 5 min), incubated in blocking solution (0.5% Triton-X100 and 10% normal donkey serum) for 1 h and then incubated 5 days for flat-mount retina and 3 days for slices at 4°C with primary antibodies in blocking solution. Primary antibodies included 1:1000 rabbit polyclonal anti-GFP with conjugated Alexa 488 (Life technologies, Carlsbad, CA, Cat. Number A-21311) and 1:1000 sheep polyclonal anti-TRPM1 (generously provided by Dr Kirill Martemyanov, Scripps Research Institute, Jupiter, FL). After incubation with primary antibody, retina pieces were rinsed with 1× PBS and then incubated with 1:1000 donkey anti-sheep Alexa Fluor 546 secondary antibody in 1× PBS (Life technologies, Carlsbad, CA, Cat. Number A-21098). Slices were incubated at room temperature for 2 h, and flat-mount retina pieces were incubated at 4°C overnight. All the retina pieces were then rinsed with 1× PBS (6 × 10 min), mounted with DAPI-containing Vectashield media (Vector Laboratories, Burlingame, CA, Inc., Cat. Number H-1200) and coverslipped. Two layers of parafilm were used as a spacer around slices, and flat-mount pieces were mounted photoreceptor side up with duct tape used as a spacer surrounding the tissue. High-magnification (20× or 40× objective) images were obtained using confocal microscopy (Olympus Fluoview FV1000 microscope equipped with Hamamatsu EM Image CCD camera). Bipolar cells that had been previously recorded from and filled with sulforhodamine (see the following section) were identified by their bright red fluorescence, which completely filled the cell as opposed to the weaker membrane-specific TRPM1 label.

Single-cell recordings

Mice were anesthetized with an intraperitoneal injection of Ringer's solution containing ketamine/xylazine (127/12 mg/kg, respectively) and killed by cervical dislocation. The eyes were enucleated and the retinas removed. Retinal slices were made and then placed in a recording chamber. Glass electrodes were filled with intracellular solution that contained Cs-gluconate

solution (20 mM CsCl, 107 mM CsOH, 107 mM D-gluconic acid, 10 mM NaHEPES, 10 mM BAPTA, 4 mM ATP and 1 mM GTP). The intracellular solution contained 1% sulforhodamine to visualize the cell and classify its morphology (64). To block inhibitory inputs, the Ames bath solution was supplemented with the following: 1 μM strychnine, 100 μM picrotoxin and 50 μM 6-tetrahydropyridin-4-yl methylphosphinic acid. L-AP4 (4 μM) was added to the bath solution to saturate mGluR6 receptors. Capsaicin (10 μM), a TRPM1 agonist, was puffed onto the rod BC dendrites to gate the opening of the TRPM1 channel. Rod BC somas were targeted for whole-cell, patch-clamp recording. Rod BCs were voltage clamped at +50 mV (25,28,65). Capsaicin (10 μM) was puffed onto the rod BC dendrites for 200 ms and 1 s durations to gate the opening of the TRPM1 channel. Three to five responses were recorded from each cell and then averaged. Prism 5.04 software (GraphPad Software) was used to perform a Kruskal–Wallis test, with a Dunn's *post hoc* test. Statistical significance is indicated as $^{**}P < 0.01$ and $^{***}P < 0.001$. Error bars report standard error of the mean. Additional methodological details are published (28).

mRNA quantification by real-time PCR

Treated and untreated eyes from *Nyx*^{nob} mice and age-matched WT controls were enucleated 4 weeks post-injection and retinas immediately dissected from the eyecup and submerged in RNA Protect (Qiagen, Inc., Valencia, CA). Retinas ($n = 1$ per condition) were homogenized in lysis buffer (Buffer RLT; RNeasy Protect Mini Kit; Qiagen, Inc.) plus βME for 45 s. RNA extraction was performed with a stabilization and purification kit (RNeasy Protect Mini Kit; Qiagen, Inc.). After measuring RNA concentration (Nanodrop, ThermoFisher, Wilmington, DE), 5μg of RNA was treated with DNase I to remove contaminating DNA (Ambion, Foster City, CA). One microgram of DNase-treated RNA was reverse transcribed (iScript cDNA synthesis kit; Bio-Rad Laboratories, Hercules, CA) and used in real-time PCR (Applied Biosystems TaqMan Gene Expression Master Mix and CFX96 PCR detection system interfaced with C1000 Touch thermal cycler; Bio-Rad Laboratories) to measure AAV-mediated *Nyx* and glyceraldehyde 3-phosphate dehydrogenase (*Gapdh*) transcripts in P2- and P30-treated *Nyx*^{nob} retinas and untreated contralateral controls.

PrimeTime mixes containing primer pairs and probe (Integrated DNA Technologies (IDT), Coralville, IA) for each transcript are included in Table 1. AAV-mediated *Nyx* primer pairs were designed to flank the 3′ *Nyx* gene and 5′ SV40 polyA and generate an amplicon of 150 bps. Internal restriction sites within the amplicon were used to cut the PCR product and analyze via electrophoresis. If the IDT pre-made set is used, this is not an issue as there is a target-specific probe that can only anneal to sequence within the amplicon. Prior to experimental data collection, PrimeTime mixes were validated according to minimum information for publication of quantitative real-time PCR experiments standards (66). Results are the average of three replicate reactions and were calculated using the $\Delta\Delta C_q$ method with signals normalized to *Gapdh* and expression relative to zero.

Supplementary Material

Supplementary Material is available at *HMG* online.

Acknowledgements

We are grateful to the Retinal Gene Therapy Vector Laboratory at the University of Florida for AAV packaging. We also acknowledge Drs Clay Smith and Kirill Martemyanov for providing GFP and TRPM1 antibodies, respectively.

Conflict of Interest statement. S.E.B., S.L.B., F.M.D. and E.M.S. are co-inventors on provisional patent, 'UF#14807-Highly Selective Transduction of ON Bipolar Cells from Intravitreal Delivered AAV Vector'. E.M.S. and C.N.D.L. are also co-inventors on US Patent 9,006,413 B2 'PCP2 Mini-Promoters'.

Funding

This work was supported by R01 EY024280 (S.E.B.), R01 140701 (M.A.M.), R01 EY12354 (R.G.G.), Genome British Columbia AGCP-CanEuCre-01 (E.M.S.), Foundation Fighting Blindness, Department of Veterans Affairs, and unrestricted grants to both the University of Florida and the University of Louisville from the Research to Prevent Blindness (RPB).

References

1. Zeitz, C., Robson, A.G. and Audo, I. (2015) Congenital stationary night blindness: an analysis and update of genotype-phenotype correlations and pathogenic mechanisms. *Prog. Retin. Eye Res.*, **45**, 58–110.
2. Miyake, Y., Yagasaki, K., Horiguchi, M., Kawase, Y. and Kanda, T. (1986) Congenital stationary night blindness with negative electroretinogram. A new classification. *Arch. Ophthalmol.*, **104**, 1013–1020.
3. Carr, R.E. (1974) Congenital stationary nightblindness. *Trans. Am. Ophthalmol. Soc.*, **72**, 448–487.
4. Dryja, T.P., McGee, T.L., Berson, E.L., Fishman, G.A., Sandberg, M.A., Alexander, K.R., Derlacki, D.J. and Rajagopalan, A.S. (2005) Night blindness and abnormal cone electroretinogram ON responses in patients with mutations in the GRM6 gene encoding mGluR6. *Proc. Natl. Acad. Sci. USA*, **102**, 4884–4889.
5. Pinto, L.H., Vitaterna, M.H., Shimomura, K., Siepka, S.M., Balannik, V., McDearmon, E.L., Omura, C., Lumayag, S., Invergo, B.M., Glawe, B. *et al.* (2007) Generation, identification and functional characterization of the nob4 mutation of Grm6 in the mouse. *Visual Neurosci.*, **24**, 111–123.
6. Masu, M., Iwakabe, H., Tagawa, Y., Miyoshi, T., Yamashita, M., Fukuda, Y., Sasaki, H., Hiroi, K., Nakamura, Y., Shigemoto, R. *et al.* (1995) Specific deficit of the ON response in visual transmission by targeted disruption of the mGluR6 gene. *Cell*, **80**, 757–765.
7. Xu, Y., Dhingra, A., Fina, M.E., Koike, C., Furukawa, T. and Vardi, N. (2012) mGluR6 deletion renders the TRPM1 channel in retina inactive. *J. Neurophysiol.*, **107**, 948–957.
8. Zeitz, C., van Genderen, M., Neidhardt, J., Luhmann, U.F., Hoeben, F., Forster, U., Wycisk, K., Matyas, G., Hoyng, C.B., Riemslag, F *et al.* (2005) Mutations in GRM6 cause autosomal recessive congenital stationary night blindness with a distinctive scotopic 15-Hz flicker electroretinogram. *Invest. Ophthalmol. Vis. Sci.*, **46**, 4328–4335.
9. Nakamura, M., Sanuki, R., Yasuma, T.R., Onishi, A., Nishiguchi, K.M., Koike, C., Kadowaki, M., Kondo, M., Miyake, Y. and Furukawa, T. (2010) TRPM1 mutations are associated with the complete form of congenital stationary night blindness. *Mol. Vis.*, **16**, 425–437.
10. Audo, I., Kohl, S., Leroy, B.P., Munier, F.L., Guillonneau, X., Mohand-Said, S., Bujakowska, K., Nandrot, E.F., Lorenz, B., Preising, M. *et al.* (2009) TRPM1 is mutated in patients with autosomal-recessive complete congenital stationary night blindness. *Am. J. Hum. Genet.*, **85**, 720–729.

11. van Genderen, M.M., Bijveld, M.M., Claassen, Y.B., Florijn, R.J., Pearring, J.N., Meire, F.M., McCall, M.A., Riemslag, F.C., Gregg, R.G., Bergen, A.A. *et al.* (2009) Mutations in TRPM1 are a common cause of complete congenital stationary night blindness. *Am. J. Hum. Genet.*, **85**, 730–736.
12. Li, Z., Sergouniotis, P.I., Michaelides, M., Mackay, D.S., Wright, G.A., Devery, S., Moore, A.T., Holder, G.E., Robson, A.G. and Webster, A.R. (2009) Recessive mutations of the gene TRPM1 abrogate ON bipolar cell function and cause complete congenital stationary night blindness in humans. *Am. J. Hum. Genet.*, **85**, 711–719.
13. Peachey, N.S., Ray, T.A., Florijn, R., Rowe, L.B., Sjoerdsma, T., Contreras-Alcantara, S., Baba, K., Tosini, G., Pozdeyev, N., Iuvone, P.M. *et al.* (2012) GPR179 is required for depolarizing bipolar cell function and is mutated in autosomal-recessive complete congenital stationary night blindness. *Am. J. Hum. Genet.*, **90**, 331–339.
14. Audo, I., Bujakowska, K., Orhan, E., Poloschek, C.M., Defoort-Dhellemmes, S., Drumare, I., Kohl, S., Luu, T.D., Lecompte, O., Zrenner, E. *et al.* (2012) Whole-exome sequencing identifies mutations in GPR179 leading to autosomal-recessive complete congenital stationary night blindness. *Am. J. Hum. Genet.*, **90**, 321–330.
15. Bech-Hansen, N.T., Naylor, M.J., Maybaum, T.A., Sparkes, R.L., Koop, B., Birch, D.G., Bergen, A.A., Prinsen, C.F., Polomeno, R.C., Gal, A. *et al.* (2000) Mutations in NYX, encoding the leucine-rich proteoglycan nyctalopin, cause X-linked complete congenital stationary night blindness. *Nat. Genet.*, **26**, 319–323.
16. Pardue, M.T., McCall, M.A., LaVail, M.M., Gregg, R.G. and Peachey, N.S. (1998) A naturally occurring mouse model of X-linked congenital stationary night blindness. *Invest Ophthalmol. Vis. Sci.*, **39**, 2443–2449.
17. Gregg, R.G., Mukhopadhyay, S., Candille, S.I., Ball, S.L., Pardue, M.T., McCall, M.A. and Peachey, N.S. (2003) Identification of the gene and the mutation responsible for the mouse nob phenotype. *Invest Ophthalmol. Vis. Sci.*, **44**, 378–384.
18. Zeitz, C., Jacobson, S.G., Hamel, C.P., Bujakowska, K., Neuille, M., Orhan, E., Zanlonghi, X., Lancelot, M.E., Michiels, C., Schwartz, S.B. *et al.* (2013) Whole-exome sequencing identifies LRIT3 mutations as a cause of autosomal-recessive complete congenital stationary night blindness. *Am. J. Hum. Genet.*, **92**, 67–75.
19. Neuille, M., El Shamieh, S., Orhan, E., Michiels, C., Antonio, A., Lancelot, M.E., Condroyer, C., Bujakowska, K., Poch, O., Sahel, J.A. *et al.* (2014) Lrit3 deficient mouse (nob6): a novel model of complete congenital stationary night blindness (cCSNB). *PLoS One*, **9**, e90342.
20. Nakajima, Y., Iwakabe, H., Akazawa, C., Nawa, H., Shigemoto, R., Mizuno, N. and Nakanishi, S. (1993) Molecular characterization of a novel retinal metabotropic glutamate receptor mGluR6 with a high agonist selectivity for L-2-amino-4-phosphonobutyrate. *J. Biol. Chem.*, **268**, 11868–11873.
21. Nomura, A., Shigemoto, R., Nakamura, Y., Okamoto, N., Mizuno, N. and Nakanishi, S. (1994) Developmentally regulated postsynaptic localization of a metabotropic glutamate receptor in rat rod bipolar cells. *Cell*, **77**, 361–369.
22. Nawy, S. (1999) The metabotropic receptor mGluR6 may signal through G(o), but not phosphodiesterase, in retinal bipolar cells. *J. Neurosci. Off. J. Soc. Neurosci.*, **19**, 2938–2944.
23. Dhingra, A., Lyubarsky, A., Jiang, M., Pugh, E.N. Jr, Birnbaumer, L., Sterling, P. and Vardi, N. (2000) The light response of ON bipolar neurons requires G[alpha]o. *J. Neurosci. Off. J. Soc. Neurosci.*, **20**, 9053–9058.
24. Morgans, C.W., Zhang, J., Jeffrey, B.G., Nelson, S.M., Burke, N. S., Duvoisin, R.M. and Brown, R.L. (2009) TRPM1 is required for the depolarizing light response in retinal ON-bipolar cells. *Proc. Natl. Acad. Sci. USA*, **106**, 19174–19178.
25. Shen, Y., Heimel, J.A., Kamermans, M., Peachey, N.S., Gregg, R. G. and Nawy, S. (2009) A transient receptor potential-like channel mediates synaptic transmission in rod bipolar cells. *J. Neurosci. Off. J. Soc. Neurosci.*, **29**, 6088–6093.
26. Koike, C., Obara, T., Uriu, Y., Numata, T., Sanuki, R., Miyata, K., Koyasu, T., Ueno, S., Funabiki, K., Tani, A. *et al.* (2010) TRPM1 is a component of the retinal ON bipolar cell transduction channel in the mGluR6 cascade. *Proc. Natl. Acad. Sci. USA*, **107**, 332–337.
27. Pearring, J.N., Bojang, P. Jr, Shen, Y., Koike, C., Furukawa, T., Nawy, S. and Gregg, R.G. (2011) A role for nyctalopin, a small leucine-rich repeat protein, in localizing the TRP melastatin 1 channel to retinal depolarizing bipolar cell dendrites. *J. Neurosci. Off. J. Soc. Neurosci.*, **31**, 10060–10066.
28. Ray, T.A., Heath, K.M., Hasan, N., Noel, J.M., Samuels, I.S., Martemyanov, K.A., Peachey, N.S., McCall, M.A. and Gregg, R.G. (2014) GPR179 is required for high sensitivity of the mGluR6 signaling cascade in depolarizing bipolar cells. *J. Neurosci. Off. J. Soc. Neurosci.*, **34**, 6334–6343.
29. Cao, Y., Posokhova, E. and Martemyanov, K.A. (2011) TRPM1 forms complexes with nyctalopin in vivo and accumulates in postsynaptic compartment of ON-bipolar neurons in mGluR6-dependent manner. *J. Neurosci. Off. J. Soc. Neurosci.*, **31**, 11521–11526.
30. Neuille, M., Morgans, C.W., Cao, Y., Orhan, E., Michiels, C., Sahel, J.A., Audo, I., Duvoisin, R.M., Martemyanov, K.A. and Zeitz, C. (2015) LRIT3 is essential to localize TRPM1 to the dendritic tips of depolarizing bipolar cells and may play a role in cone synapse formation. *Eur. J. Neurosci.*, **42**, 1966–1975.
31. Bainbridge, J.W., Smith, A.J., Barker, S.S., Robbie, S., Henderson, R., Balaggan, K., Viswanathan, A., Holder, G.E., Stockman, A., Tyler, N. *et al.* (2008) Effect of gene therapy on visual function in Leber's congenital amaurosis. *N. Engl. J. Med.*, **358**, 2231–2239.
32. Banin, E., Bandah-Rozenfeld, D., Obolensky, A., Cideciyan, A. V., Aleman, T.S., Marks-Ohana, D., Sela, M., Boye, S., Sumaroka, A., Roman, A.J. *et al.* (2010) Molecular anthropology meets genetic medicine to treat blindness in the North African Jewish population: human gene therapy initiated in Israel. *Hum. Gene Ther.*, **21**, 1749–1757.
33. Boye, S.E., Boye, S.L., Lewin, A.S. and Hauswirth, W.W. (2013) A comprehensive review of retinal gene therapy. *Mol. Ther.*, **21**, 509–519.
34. Cideciyan, A.V., Aleman, T.S., Boye, S.L., Schwartz, S.B., Kaushal, S., Roman, A.J., Pang, J.J., Sumaroka, A., Windsor, E.A., Wilson, J.M. *et al.* (2008) Human gene therapy for RPE65 isomerase deficiency activates the retinoid cycle of vision but with slow rod kinetics. *Proc. Natl. Acad. Sci. USA*, **105**, 15112–15117.
35. Jacobson, S.G., Cideciyan, A.V., Ratnakaram, R., Heon, E., Schwartz, S.B., Roman, A.J., Peden, M.C., Aleman, T.S., Boye, S.L., Sumaroka, A. *et al.* (2012) Gene therapy for Leber congenital amaurosis caused by RPE65 mutations: safety and efficacy in 15 children and adults followed up to 3 years. *Arch. Ophthalmol.*, **130**, 9–24.
36. MacLaren, R.E., Groppe, M., Barnard, A.R., Cottriall, C.L., Tolmachova, T., Seymour, L., Clark, K.R., During, M.J., Cremers, F.P., Black, G.C. *et al.* (2014) Retinal gene therapy in patients with choroideremia: initial findings from a phase 1/2 clinical trial. *Lancet*, **383**, 1129–1137.

37. Maguire, A.M., Simonelli, F., Pierce, E.A., Pugh, E.N. Jr, Mingozzi, F., Bennicelli, J., Banfi, S., Marshall, K.A., Testa, F., Surace, E.M. *et al.* (2008) Safety and efficacy of gene transfer for Leber's congenital amaurosis. *N. Engl. J. Med.*, **358**, 2240–2248.
38. Dalkara, D., Kolstad, K.D., Caporale, N., Visel, M., Klimczak, R. R., Schaffer, D.V. and Flannery, J.G. (2009) Inner limiting membrane barriers to AAV-mediated retinal transduction from the vitreous. *Mol. Ther.*, **17**, 2096–2102.
39. Kay, C.N., Ryals, R.C., Aslanidi, G.V., Min, S.H., Ruan, Q., Sun, J., Dyka, F.M., Kasuga, D., Ayala, A.E., Van, V.K. *et al.* (2013) Targeting photoreceptors via intravitreal delivery using novel, capsid-mutated AAV vectors. *PLoS One*, **8**, e62097.
40. Doroudchi, M.M., Greenberg, K.P., Liu, J., Silka, K.A., Boyden, E. S., Lockridge, J.A., Arman, A.C., Janani, R., Boye, S.E., Boye, S.L. *et al.* (2011) Virally delivered channelrhodopsin-2 safely and effectively restores visual function in multiple mouse models of blindness. *Mol. Ther.*, **19**, 1220–1229.
41. Mace, E., Caplette, R., Marre, O., Sengupta, A., Chaffiol, A., Barbe, P., Desrosiers, M., Bamberg, E., Sahel, J.A., Picaud, S. *et al.* (2015) Targeting channelrhodopsin-2 to ON-bipolar cells with vitreally administered AAV Restores ON and OFF visual responses in blind mice. *Mol. Ther.*, **23**, 7–16.
42. Cronin, T., Vandenberghe, L.H., Hantz, P., Juttner, J., Reimann, A., Kacso, A.E., Huckfeldt, R.M., Busskamp, V., Kohler, H., Lagali, P.S. *et al.* (2014) Efficient transduction and optogenetic stimulation of retinal bipolar cells by a synthetic adeno-associated virus capsid and promoter. *EMBO Mol. Med.*, **6**, 1175–1190.
43. Gaub, B.M., Berry, M.H., Holt, A.E., Reiner, A., Kienzler, M.A., Dolgova, N., Nikonov, S., Aguirre, G.D., Beltran, W.A., Flannery, J.G. *et al.* (2014) Restoration of visual function by expression of a light-gated mammalian ion channel in retinal ganglion cells or ON-bipolar cells. *Proc. Natl. Acad. Sci. USA*, **111**, E5574–E5583.
44. van Wyk, M., Pielecka-Fortuna, J., Lowel, S. and Kleinlogel, S. (2015) Restoring the ON Switch in Blind Retinas: Opto-mGluR6, a next-generation, cell-tailored optogenetic tool. *PLoS Biol.*, **13**, e1002143.
45. de Leeuw, C.N., Dyka, F.M., Boye, S.L., Laprise, S., Zhou, M., Chou, A.Y., Borretta, L., McInerny, S.C., Banks, K.G., Portales-Casamar, E. *et al.* (2014) Targeted CNS delivery using human MiniPromoters and demonstrated compatibility with adeno-associated viral vectors. *Mol. Ther. Methods Clin. Dev.*, **1**, 5.
46. Gregg, R.G., Kamermans, M., Klooster, J., Lukasiewicz, P.D., Peachey, N.S., Vessey, K.A. and McCall, M.A. (2007) Nyctalopin expression in retinal bipolar cells restores visual function in a mouse model of complete X-linked congenital stationary night blindness. *J. Neurophysiol.*, **98**, 3023–3033.
47. Bahadori, R., Biehlmaier, O., Zeitz, C., Labhart, T., Makhankov, Y.V., Forster, U., Gesemann, M., Berger, W. and Neuhauss, S.C. (2006) Nyctalopin is essential for synaptic transmission in the cone dominated zebrafish retina. *Eur. J. Neurosci.*, **24**, 1664–1674.
48. Morgans, C.W., Ren, G. and Akileswaran, L. (2006) Localization of nyctalopin in the mammalian retina. *Eur. J. Neurosci.*, **23**, 1163–1171.
49. Pesch, K., Zeitz, C., Fries, J.E., Munscher, S., Pusch, C.M., Kohler, K., Berger, W. and Wissinger, B. (2003) Isolation of the mouse nyctalopin gene NYX and expression studies in mouse and rat retina. *Invest Ophthalmol. Vis. Sci.*, **44**, 2260–2266.
50. Shirato, S., Maeda, H., Miura, G. and Frishman, L.J. (2008) Post-receptoral contributions to the light-adapted ERG of mice lacking b-waves. *Exp. Eye Res.*, **86**, 914–928.
51. Peachey, N.S., Pearring, J.N., Bojang, P. Jr, Hirschtritt, M.E., Sturgill-Short, G., Ray, T.A., Furukawa, T., Koike, C., Goldberg, A.F., Shen, Y. *et al.* (2012) Depolarizing bipolar cell dysfunction due to a Trpm1 point mutation. *J. Neurophysiol.*, **108**, 2442–2451.
52. Rapaport, D.H., Wong, L.L., Wood, E.D., Yasumura, D. and LaVail, M.M. (2004) Timing and topography of cell genesis in the rat retina. *J. Comp. Neurol.*, **474**, 304–324.
53. Cepko, C. (2014) Intrinsically different retinal progenitor cells produce specific types of progeny. *Nat. Rev. Neurosci.*, **15**, 615–627.
54. Hubel, D.H., Wiesel, T.N. and LeVay, S. (1977) Plasticity of ocular dominance columns in monkey striate cortex. *Philos. Trans. R. Soc. London, Ser. B*, **278**, 377–409.
55. Dunn, F.A., Della Santina, L., Parker, E.D. and Wong, R.O. (2013) Sensory experience shapes the development of the visual system's first synapse. *Neuron*, **80**, 1159–1166.
56. Chakraborty, R., Park, H.N., Hanif, A.M., Sidhu, C., Iuvone, P.M. and Pardue, M.T. (2015) ON pathway mutations increase susceptibility to form-deprivation myopia. *Exp. Eye Res.*, **137**, 79–83.
57. Pardue, M.T., Faulkner, A.E., Fernandes, A., Yin, H., Schaeffel, F., Williams, R.W., Pozdeyev, N. and Iuvone, P.M. (2008) High susceptibility to experimental myopia in a mouse model with a retinal on pathway defect. *Invest Ophthalmol. Vis. Sci.*, **49**, 706–712.
58. Sarnaik, R., Chen, H., Liu, X. and Cang, J. (2014) Genetic disruption of the on visual pathway affects cortical orientation selectivity and contrast sensitivity in mice. *J. Neurophysiol.*, **111**, 2276–2286.
59. Portales-Casamar, E., Swanson, D.J., Liu, L., de Leeuw, C.N., Banks, K.G., Ho Sui, S.J., Fulton, D.L., Ali, J., Amirabbasi, M., Arenillas, D.J. *et al.* (2010) A regulatory toolbox of MiniPromoters to drive selective expression in the brain. *Proc. Natl. Acad. Sci. USA*, **107**, 16589–16594.
60. Jacobson, S.G., Acland, G.M., Aguirre, G.D., Aleman, T.S., Schwartz, S.B., Cideciyan, A.V., Zeiss, C.J., Komaromy, A.M., Kaushal, S., Roman, A.J. *et al.* (2006) Safety of recombinant adeno-associated virus type 2-RPE65 vector delivered by ocular subretinal injection. *Mol. Ther.*, **13**, 1074–1084.
61. Zolotukhin, S., Potter, M., Zolotukhin, I., Sakai, Y., Loiler, S., Fraites, T.J. Jr, Chiodo, V.A., Phillipsberg, T., Muzyczka, N., Hauswirth, W.W. *et al.* (2002) Production and purification of serotype 1, 2, and 5 recombinant adeno-associated viral vectors. *Methods*, **28**, 158–167.
62. Jacobson, S.G., Boye, S.L., Aleman, T.S., Conlon, T.J., Zeiss, C.J., Roman, A.J., Cideciyan, A.V., Schwartz, S.B., Komaromy, A.M., Doobrajh, M. *et al.* (2006) Safety in nonhuman primates of ocular AAV2-RPE65, a candidate treatment for blindness in Leber congenital amaurosis. *Hum. Gene Ther.*, **17**, 845–858.
63. Boye, S.E., Boye, S.L., Pang, J., Ryals, R., Everhart, D., Umino, Y., Neeley, A.W., Besharse, J., Barlow, R. and Hauswirth, W.W. (2010) Functional and behavioral restoration of vision by gene therapy in the guanylate cyclase-1 (GC1) knockout mouse. *PLoS One*, **5**, e11306.
64. Ghosh, K.K., Bujan, S., Haverkamp, S., Feigenspan, A. and Wassle, H. (2004) Types of bipolar cells in the mouse retina. *J. Comp. Neurol.*, **469**, 70–82.
65. Nawy, S. (2004) Desensitization of the mGluR6 transduction current in tiger salamander on bipolar cells. *J. Physiol.*, **558**, 137–146.
66. Bustin, S.A., Benes, V., Garson, J.A., Hellemans, J., Huggett, J., Kubista, M., Mueller, R., Nolan, T., Pfaffl, M.W., Shipley, G.L. *et al.* (2009) The MIQE guidelines: minimum information for publication of quantitative real-time PCR experiments. *Clin. Chem.*, **55**, 611–622.